EJN European Journal of Neuroscience

FENS Federation of European Neuroscience Societies

European Journal of Neuroscience, Vol. 43, pp. 516–528, 2016 doi:10.1111/ejn.13136

COGNITIVE NEUROSCIENCE

Facilitative effect of repetitive presentation of one stimulus on cortical responses to other stimuli in macaque monkeys – a possible neural mechanism for mismatch negativity

Kana Takaura and Naotaka Fujii
Laboratory for Adaptive Intelligence, RIKEN Brain Science Institute, 2-1 Hirosawa, Wako-shi, Siatama 351-0198, Japan

Keywords: adaptation, auditory, electrocorticogram, roving oddball paradigm

Edited by John Foxe
Received 17 July 2015, revised 14 November 2015, accepted 20 November 2015

Abstract

The event-related potential 'mismatch negativity' (MMN) is an indicator of a perceiver's ability to detect deviations in sensory signal streams. MMN and its homologue in animals, mismatch activity (MMA), are differential neural responses to a repeatedly presented stimulus and a subsequent deviant stimulus (oddball). Because neural mechanisms underlying MMN and MMA remain unclear, there is a controversy as to whether MMN and MMA arise solely from stimulus-specific adaptation (SSA), in which the response to a stimulus cumulatively attenuates with its repetitive presentation. To address this issue, we used electrocorticography and the auditory roving-oddball paradigm in two awake macaque monkeys. We examined the effect of stimulus repetition number on MMA and on responses to repeated stimuli and oddballs across the cerebral cortex in the time–frequency domain. As the repetition number increased, MMA spread across the temporal, frontal and parietal cortices, and each electrode yielded a larger MMA. Surprisingly, this increment in MMA largely depended on response augmentation to the oddball rather than on SSA to the repeated stimulus. Following sufficient repetition, the oddball evoked a spectral power increment in some electrodes on the frontal cortex that had shown no power increase to the stimuli with less or no preceding repetition. We thereby revealed that repetitive presentation of one stimulus not only leads to SSA but also facilitates the cortical response to oddballs involving a wide range of cortical regions. This facilitative effect might underlie the generation of MMN-like scalp potentials in macaques that potentially shares similar neural mechanisms with MMN in humans.

Introduction

The ability to detect aberrations in regularized sensory signal streams is fundamental for adaptive behaviors, but its neural underpinnings are poorly understood. One related neural signature is an event-related potential called 'mismatch negativity' (MMN), first discovered in electroencephalographic (EEG) studies of humans (Naatanen *et al.*, 1978). Traditionally, MMN is recorded with the auditory oddball sequence, wherein infrequent (Deviant; synonymous here with 'oddball') auditory stimuli are randomly embedded in sequences of a regularly repeated and frequent (Standard) stimulus. Subtracting the neural response to Standard stimuli from that to Deviant stimuli yields MMN, which is observable regardless of a subject's attention to the stimuli or any behavioral tasks (Naatanen *et al.*, 2012).

One unresolved issue concerning the neural mechanisms of MMN is whether or not stimulus-specific adaptation (SSA) can solely explain MMN. SSA is a phenomenon in which the neural response attenuates with repetitive presentation of a stimulus (Fruhstorfer *et al.*, 1970; Desimone, 1996). The nature of SSA and its involvement in MMN has been investigated with animal models in the primary auditory cortex (AI) and subcortical structures. While SSA to Standard stimuli is thought to play a key role in MMN generation (Ulanovsky *et al.*, 2003; Perez-Gonzalez *et al.*, 2005; Malmierca *et al.*, 2009; Antunes *et al.*, 2010), several studies have implied additional mechanisms (Javitt *et al.*, 1996; Farley *et al.*, 2010; Taaseh *et al.*, 2011). Javitt *et al.* (1996) proposed that stimulus repetition increases inhibition of neurons sensitive to the repeated stimulus and decreases the level of inhibition of other neurons that are insensitive to the stimulus. This notion of a release from inhibition has much less empirical support than increased inhibition or response attenuation (i.e., SSA).

The present study therefore sought to determine whether there is evidence of this mechanism by examining the effect of stimulus repetition number on the cortical response to auditory stimuli by electrocorticogram (ECoG) recording in non-human primates

Correspondence: Naotaka Fujii, as above.
E-mail: na@brain.riken.jp

exposed to the roving-oddball sequence. If stimulus repetition decreases inhibition of neurons not sensitive to the repeated stimulus, the population response to Deviant stimuli would be facilitated by an increase in the number of preceding Standard stimuli. We also assessed the stimulus repetition effect on the cortical responsiveness to the auditory stimuli, using a 'many-standards condition' in which the stimuli were presented without preceding repetition. While our principal focus was to decipher the effect of stimulus repetition on the cortical response to auditory stimuli, our findings have potential implications for how mismatch activity (MMA) and MMN are generated (see Discussion). However, the present study did not aim to test the current theoretical models of MMN.

There are several technical advantages of our approach compared to traditional EEG experiments. ECoG signal has better spatial resolution than EEG and contains high-frequency signals associated with population-spiking activity around the electrode (Kayser *et al.*, 2007; Ray *et al.*, 2008; Ray & Maunsell, 2011). Furthermore, in animal models we can simultaneously record ECoG signals from widespread cortical regions using chronically implanted electrodes (Nagasaka *et al.*, 2011). These advantages enable us to explore the repetition-number effect that is potentially overlooked with other recording modalities.

Materials and methods

All experimental procedures were performed in accordance with the experimental protocols of the RIKEN Ethics Committee and were in accordance with the National Institutes of Health Guide for the Care and Use of Laboratory Animals. All procedures were approved by the Committee for Animal Experiment at RIKEN (No. H24-2-2-3 (4)) and were in accordance with the National Institutes of Health Guide for the Care and Use of Laboratory Animals.

Subjects and experimental set-up

Two macaque monkeys, identified as C (male, 7.5 kg) and Q (male, 8.8 kg), were used in the experiments after brain magnetic resonance images (MRIs) were acquired. Before the monkeys were implanted with subdural ECoG electrodes, they were familiarized with the monkey chair and experimental settings. The monkeys sat in a primate chair in a dark, electrically shielded and sound-attenuated chamber with their head fixed in a position with a custom-made helmet. For auditory stimuli, we positioned a pair of audio speakers (Fostex, Japan) on the right and left sides, at a distance of ~ 80 cm from the head. We used MATLAB® (Mathworks, Natick, MA, USA) and Psychophysics Toolbox (Brainard, 1997; Pelli, 1997) to present auditory stimuli.

Electrode implantation

Subdural electrodes were surgically implanted. The monkeys were anesthetized by administration of atropine (0.05 mg/kg, intramuscular), ketamine (5 mg/kg, intramuscular) and pentobarbital (20 mg/kg, intravenous). Throughout surgery we monitored the heart rate, blood pressure, body temperature, SpO2 (peripheral capillary oxygen saturation), and reflex response to noxious stimulation, adjusting the dose of pentobarbital accordingly. In the subdural space we chronically implanted a customized multichannel ECoG electrode array (Unique Median, Japan; Nagasaka *et al.*, 2011), embedded with 2.1-mm-diameter platinum electrodes (1-mm diameter exposed from a silicone sheet). The center-to-center inter-electrode distance was 5 mm. Both monkeys were implanted with 128 ECoG electrodes, a reference electrode in the subdural space and a ground electrode in the epidural space above the right hemisphere (the reference and ground electrodes were 5-mm × 10-mm rectangular platinum plates). To localize the electrodes, we acquired post-operative X-ray images and co-registered them with the MRIs (Fig. 1A). We manually identified the location of each electrode by projecting the electrodes in the X-ray images onto the cortical surface reconstructed from the MRIs. In Fig. 1A we depict implanted electrodes on the dorsal and ventral surfaces with tilted orientations to indicate the cortical curvature of those areas. For monkey Q, 10 electrodes are shown beneath the orbitofrontal cortex outside the cortical boundary. Colors represent the grouping of the electrodes for Table 1. We roughly classified the electrodes into six groups, e.g. three groups in the frontal lobe (prefrontal cortex, orbitofrontal cortex and pre-motor cortex), parietal cortex, temporal cortex and occipital cortex, based on the electrode locations relative to anatomical landmarks. Note that we classified the electrodes into six groups to concisely summarize the results shown in Fig. 3, and thus the classification may not be strictly correct. For example, we classified some electrodes on the anterior bank of the central sulcus (presumably on the primary motor cortex) into the group 'pre-motor cortex'.

Stimulus design and data acquisition

ECoG signals were recorded while the monkeys were passively exposed to the auditory stimulus sequences (passive condition), which is a typical condition in human subjects studies of MMN. We used two types of auditory stimulus sequences: a roving-oddball sequence (Baldeweg *et al.*, 2004; Haenschel *et al.*, 2005; Garrido *et al.*, 2009; Costa-Faidella *et al.*, 2011; Schmidt *et al.*, 2012) and a control sequence. In the roving-oddball sequence, trains of pure tones of the same pitch separated by a fixed inter-tone interval were presented without any inter-train interval, and each train was followed by another train of tones that differed in pitch (Fig. 1B). The number of tones in each train was 3, 5 or 11, and we used 20 kinds of pure sinusoidal tones of 64 ms duration, including a 7-ms rise and a 7-ms fade time, separated by 1/4 octave, in the range 250–6277 Hz (average intensity 65 dB SPL). Thus, each roving-oddball sequence contained 3 × 20 trains of pure tones. The order of the frequency for the trains was randomized within each block of 20 trains so that a train of a certain frequency was separated from another train of the same frequency by 19 trains of other frequencies, on average. Then, the order of the tone number for the trains was pseudo-randomly defined. We took the last tone in the train of n repetitions (n = 3, 5, 11) and the first tone in the subsequent train as a pair of Standard and Deviant stimuli for the condition of n-repetitions. Thus, theoretically, once a given stimulus served as Standard, the stimulus appeared as Deviant after 19 × (3 + 5 + 11)/3 = 120 tones (~ 60 s) and once a given stimulus served as a Deviant, the stimulus appeared as a Deviant after 20 × (3 + 5 + 11)/3 = 127 tones (~ 64 s; inter-deviant time interval, IDI), on average. Note that this holds true for almost all Deviants regardless of the number of tones in the preceding train or the condition. Figure 1C shows the distributions of IDIs in the actual dataset. For the first presentation of each stimulus in one session, we counted the number of tones preceding the stimulus. The distributions of IDIs were not significantly different across the conditions (one-way ANOVA, P = 0.043, F_2 = 3.14, but no paired comparisons reached the criteria of significance in the *post hoc* two-sided tests with Bonferroni correction for monkey C; P = 0.20, F_2 = 1.64 for monkey Q). Figure 1D shows the distributions of the magnitude of pitch differences between Standard and Deviant stimuli. They were not statistically significantly different among the conditions in either monkey

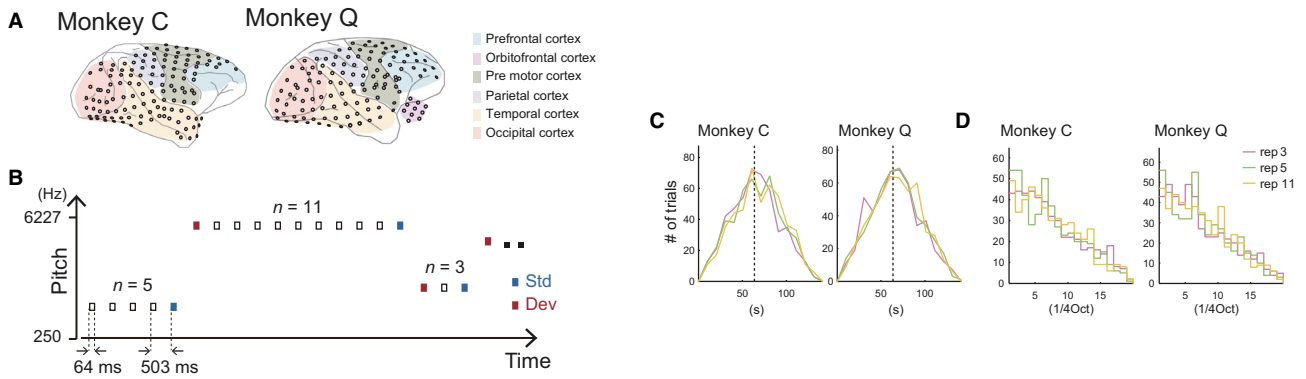

FIG. 1. Experimental design. (A) Locations of the 128 subdural electrodes in each monkey. In monkey Q, 10 electrodes were located under the orbitofrontal cortex. Colors indicate the groups of electrodes defined in Table 1. (B) Schematic of the roving-oddball sequence. One sequence consisted of 60 trains of pure tones (20 frequencies × 3 types of repetition number). We took the last tone in each train of *n*-tones (*n* = 3, 5 or 11) and the first tone of the subsequent train as a pair of Standard and Deviant stimuli for the condition of *n*-repetitions. (C) Distribution of the IDI (see Methods). (D) Distributions of the pitch differences between Standard and Deviant stimuli. In (C) and (D), purple, green and yellow lines indicate the 3-, 5- and 11-repetitions conditions respectively. Std, Standard; Dev, Deviant.

TABLE 1. Number *n* of electrodes showing significant MMA

	Monkey C						Monkey Q					
	Rep3		Rep 5		Rep 11		Rep 3		Rep 5		Rep 11	
	n	Prop	*n*	Prop	*n*	Prop	*n*	Prop	*n*	Prop	*n*	Prop
Prefrontal	3	0.27	1	0.09	7	0.64	11	0.61	7	0.39	14	0.78
Orbitofrontal	0	–	0	–	0	–	5	0.50	5	0.50	10	1.00
Pre-motor	14	0.42	14	0.42	19	0.67	11	0.37	9	0.33	16	0.53
Parietal	4	0.33	6	0.5	8	0.67	1	0.08	0	0	7	0.54
Temporal	17	0.43	21	0.53	22	0.55	11	0.44	14	0.56	16	0.64
Occipital	4	0.13	4	0.13	1	0.03	1	0.03	8	0.25	12	0.38

Prop, *n* as a proportion of the total number of the electrodes in each area. For monkey C, no electrode was classified in the orbitofrontal cortex.

($0.4 < P$, $F_2 < 1$). Therefore, the difference in the cortical activity across the conditions cannot be attributed to the difference in pitch between Standard and Deviant stimuli. To balance the number of Standard and Deviant stimuli, we added one tone differing in pitch from the last train at the end of the sequence, resulting in 381 tones in one roving-oddball sequence. The stimulus onset asynchrony was 503 ms and the overall probability of each tone in one sequence was ~ 5% (19/381). As a control sequence we adopted the many-standards condition (Jacobsen & Schroger, 2001; Farley *et al.*, 2010; Fishman & Steinschneider, 2012). We presented the 20 types of pure tones comprising the roving-oddball sequence with the same stimulus onset asynchrony as the oddball sequence in the pseudorandom order so that the overall probability of each tone in the control sequence was equal to that in the roving-oddball sequence (5%). We considered all tones in the control sequence as Controls. The starting time of each stimulus sequence and ECoG signals were recorded at 1 kHz by using a Cerebus Data Acquisition System (Blackrock Microsystems, Salt Lake City, UT, USA).

Experimental data were obtained over 5 and 4 days for monkey C and monkey Q, respectively. We presented one control sequence and/or four oddball sequences in one experimental session. In total, we recorded ECoG signals for six sessions in each monkey. When we conducted more than two sessions in 1 day, the sessions were separated by 30 min during which time the monkeys performed another experiment involving a fixation visual stimuli task. When we collected the data for the present study, the display for the fixation task was turned off and the equipment to deliver the reward was removed.

Data analysis

Pre-processing and transformation into the time–frequency domain

We removed 50-Hz line noise from the continuous ECoG data in each channel using the multi-taper method implemented as a MATLAB® function (rmlinesc.m) in an open-source Chronux Toolbox (http://chronux.org; Mitra & Bokil, 2008) and resampled the data to 500 Hz. From the cleaned continuous data, we extracted 1709-ms epochs beginning 503 ms before the onset of the Standard for the roving-oddball sequence and 1208-ms epochs beginning 503 ms before the stimulus onset for the control sequence. We re-referred the signals with respect to the median across all electrodes at each time point. We extracted 1006-ms epochs starting 503 ms before each stimulus onset and defined each epoch as one trial, for Standard, Deviant and Control, respectively. For event-related potential (ERP) analysis, we corrected the baseline by subtracting the mean across time points then averaged the signal across trials. Figure 2A (right panel) shows an example of ERPs recorded from one electrode on the temporal cortex (left panel).

We examined the effect of repetition number in the time–frequency domain to take advantage of the property that ECoG signals contain high-frequency activity (> 80 Hz) associated with spiking

activity of the population near the electrode (Kayser *et al.*, 2007; Ray *et al.*, 2008; Ray & Maunsell, 2011). We estimated the spectrogram using the multi-taper method, where a half-bandwidth (W) is defined by W = (tp + 1)/2*T*, with tp and *T* being the number of tapes and the size of the time window in s (Mitra & Bokil, 2008). We used tp = 2 and *T* = 0.18 s, resulting in a half-bandwidth of 8.3 Hz. We estimated the time-course of the spectral power by sliding the time-window by 4 ms. We obtained a single-trial estimate of the power spectrogram up to 150 Hz. The number of trials was 1440 each for Standard and Deviant (480 for each condition) and 480 for Control. In each trial, we subtracted the median across time at each frequency point to remove the overall trend in each trial. We then normalized the power with *z*-score transformation at each frequency point, using the median and interquartile range across all time points of the Standard, Deviant and Control stimuli. Figure 2B shows example spectrograms for Standard (left panel) and Deviant (right panel) trials after normalization. We normalized the Standard, Deviant and Control trials using the same values (the median and interquartile range across all the time-points in all trials) to avoid a bias potentially inherent in the normalization techniques with a pre-stimulus baseline period. If any pre-stimulus modulation exists and if such a modulation is specific to one experimental condition, the normalization procedure with pre-stimulus baseline would cause an artificial difference across the conditions, which could affect the comparison of the strength of the response across the conditions (see next section on MMA). We avoided this potential artifact by calculating a *z*-score for all conditions.

MMA and response to Standard and Deviant stimuli

In each condition and for each electrode, we assessed the significance of the difference between the Standard and Deviant trials using the cluster-based correction for multiple comparisons (Maris & Oostenveld, 2007). This cluster-based analysis allowed us to determine significant differences without any assumption about the time–frequency distribution of the cortical activity. We subtracted the normalized power in Standard trials from that in Deviant trials at each time and frequency point and calculated the median across the trials (see example in Fig. 2C, left panel), which we abbreviated to DS_0. We generated the null distribution of the difference by shuffling a half of the Standard and Deviant trials (240 = 480/2) 1000 times, which we abbreviated DS_i (i = 1 . . . 1000). At each time and frequency point in the 300-ms epoch just after stimulus onset, we transformed DS_i (i = 0 . . . 1000) into a *z*-score, using the median and interquartile range across 1001 samples. Then, we corrected for multiple comparisons over time and frequency using a nonparametric cluster-based method (Maris & Oostenveld, 2007). In each DS_i, we gathered all time and frequency points with *z*-scores corresponding to *P*-values < 0.025 or > 0.975 into one cluster based on adjacency in time and frequency, and calculated cluster-level statistics by considering the sum of the *z*-scores within each cluster. We took the smallest or largest cluster-level statistics as a representative value of DS_i. We regarded DS_0 as significant when the cluster-level statistics of DS_0 were in the top or bottom 2.5% of the cluster-level statistics of DS_i (i = 1. . .1000). An example of a significant cluster is shown in Fig. 2C (right panel). We obtained empirical *P*-values by taking the proportion of the samples with larger or smaller cluster-level statistics than SD_0. When we identified electrodes with significant MMA, we additionally corrected for multiple comparisons with the false-discovery rate (FDR) at q = 0.05 (Benjamini & Hochberg, 1995) across electrodes and conditions. We examined both significant increment and significant decrement in power in Deviant trials compared with Standard trials and found that the decrement in power did not survive the FDR correction in any electrodes and in any conditions. Thus, we conducted the following analysis on the strengths of MMA and of the response to Standard and Deviant stimuli only for electrodes with a significant increment in Deviant trials in any one condition.

To quantify the strength of MMA, we defined the region of interest in the time–frequency space for each electrode as all the time–frequency points incorporated in any significant cluster for the three conditions. Within the region of interest, we calculated the sum of the difference in the normalized power between Standard and Deviant trials in each pair of the trials and for each condition. We also quantified the strength of the responses to Standard and Deviant stimuli by calculating the sum of the normalized power within the region of interest in Standard and Deviant trials within each condition. We assessed the repetition number effect on the strength of MMA and the strength of the response to Standard and Deviant stimuli, using Friedman's test (α = 0.05) with FDR correction (q = 0.05) and a *post hoc* two-sided sign test (α = 0.05) at the population level (across the electrodes) and at the single-electrode level.

Responsiveness to Deviant and Control stimuli

To further examine the effect of the stimulus repetition on the cortical response to Deviant stimuli, we assessed the responsiveness of each electrode to Deviants, and to the Control stimuli that were physically identical to Deviant stimuli but presented without preceding repetition. We defined the 'responsiveness' based on whether or not a sig-

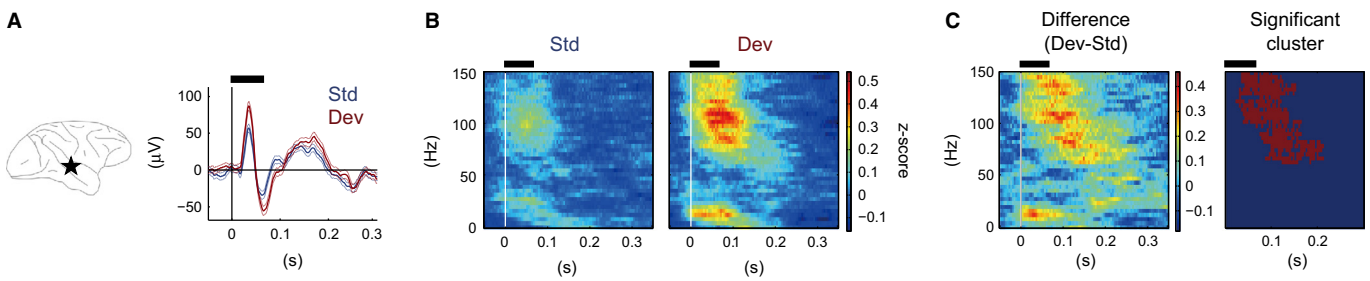

FIG. 2. Examples of neural responses in Standard and Deviant trials. (A) Location of an example electrode (left panel) and ERPs (right panel) for Standard (blue lines) and Deviant (red lines) trials in the 5-repetitions condition. The dashed lines indicate the SE across the trials. (B) Spectrograms for Standard (left panel) and Deviant (right panel) trials. (C) Difference between the responses to Standard and Deviant (left panel) stimuli, and the significant cluster (right panel) defined by the cluster-based correction for multiple comparisons across the time and frequency points. The black horizontal bar above each panel indicates the epoch when the tones were presented. ERP, event-related potential; Std, Standard; Dev, Deviant.

nificant power increase or decrease occurred in comparing the spectral powers before and after the stimulus onset. We compared the post-stimulus activity in the 0.3-s epoch just after stimulus onset (75 time-points) to the baseline matrix. To generate the baseline matrix, we first calculated the mean normalized power for the 0.05 s just before stimulus onset at each frequency point in each trial, resulting in one vector for each trial. We then created a matrix copying the vector 75 times and took the resultant matrix as a baseline matrix of each trial. We made the baseline matrix of the same size as the post-stimulus activity so that we could conduct cluster-based analysis that allowed us to compare the cortical activity before and after the stimulus onset without any assumptions regarding the time and frequency distribution of the auditory response (see Data analysis subsection MMA above for details on the cluster-based analysis). We calculated the difference of the normalized power at each time and frequency point between the post-stimulus and baseline matrix and assessed the significance by generating the null distribution ($N = 1000$).

Results

Repetition-number effect on the distribution of MMA

First, we defined which electrodes showed MMA for each condition and examined the repetition-number effect on the spatial distribution of MMA. Figure 2 shows an example of the response to the Standard and Deviant (B) and MMA (C) in the time–frequency domain. Because the decrement in the spectral power did not survive FDR correction in any electrodes and in any conditions, hereafter we refer to the significant increment in the spectral power in Deviant trials compared with Standard trials as MMA.

We observed a facilitative effect of stimulus repetition on the distribution of MMA. As the number of stimulus repetitions increased, MMA was observed in more widely distributed cortical regions and the MMA of each electrode became statistically robust. Figure 3 summarizes the effect of the stimulus repetition on the distribution of the electrodes with MMA (A and D), the proportion of the electrodes with MMA (B and E) and the time–frequency pattern of MMA as a population (C and F). When the stimulus was repeated three times (the rep 3 condition, top panels in A and D), MMA occurred mainly in the electrodes on the temporal cortex and additionally in the dorsal part of the frontal cortex, although they were sparse in monkey C. When the stimulus was repeated 11 times (the rep 11 condition, bottom panels in A and D), MMA in the frontal cortex became statistically stronger (larger circles in bottom panel compared with smaller circles in the top panels of Figs 3A and D) and MMA emerged in more electrodes, spreading over the dorsal and ventral part of the premotor cortex and around the intraparietal sulcus in both monkeys.

As expected from these observations, the proportion of electrodes with MMA increased as a function of repetition number (Figs 3B and E). The proportions of the electrodes with MMA were 33, 36 and 45% in monkey C and 31, 34 and 59% in monkey Q, for each repetition number or condition. Table 1 shows the number of the electrodes with MMA in each cortical area (see the color code in Fig. 1A). As shown in the inset below the panel for the 11-repetitions condition described in Figs 3C and F, MMA as a population was in the range 0–0.2 s after the stimulus onset and peaked at ~ 0.1 s in both monkeys, which is compatible with previous studies of MMA in primates (Javitt *et al.*, 1992, 1994, 1996; Gil-da-Costa *et al.*, 2013). MMA in the time–frequency domain comprised two components. One was in the low-frequency range below ~ 30 Hz and another was in the high-frequency range > 80 Hz. In monkey Q, MMA that was observed in the lower frequency range in the 3-repetitions condition (Fig. 3F, top panel) disappeared in the 5-repetitions condition (Fig. 3F, middle panel), because the cluster with the strongest statistical power shifted from the low- to high-frequency component in the electrodes with MMA in the 3-repetitions condition. We also examined the effect of repetition number on ERPs by the same cluster-based method used in the frequency domain analysis, but we did not discern a coherent pattern that was consistent between the monkeys (data is not shown).

Repetition-number effect on the strengths of MMA and of the responses to Standard and Deviant stimuli

Next, we investigated the effect of stimulus repetition on the strength of both MMA and the response to Standard and Deviant stimuli, focusing on the electrodes that showed significant MMA in any one of the conditions (78 electrodes for monkey C and 89 electrodes for monkey Q). For each electrode, we quantified 3 measures in each condition (see Data analysis subsection MMA above for details) and compared them across the conditions at the single-electrode and population levels.

We observed a significant increment in MMA that was mainly due to an augmentation of the response to Deviant stimuli rather than to an attenuation of the response to Standard stimuli. Figures 4A and B shows an example of the response to Standard and Deviant stimuli, and the difference between them (Fig. 4C) in each condition. As for ERPs (Fig. 4A, middle and bottom panels), only the 11-repetitions condition (yellow lines) showed differences from the other conditions (i.e., in the peak ~ 50 ms in Standard trials and in the late component after 150 ms in Deviant trials), and these were slight. ERPs in the 3- (light gray lines) and 5-repetitions (dark gray lines) conditions were nearly the same in Standard and Deviant trials. On the other hand, in the time–frequency domain (Figs 4B and C) we observed that the high-frequency component above 70–80 Hz that was observed ~ 100 ms after stimulus onset become stronger with increase in the number of stimulus repetitions, both in the response to Deviant stimuli (Fig. 4B, right column) and in the difference between Standard and Deviant trials (Fig. 4C). In this example electrode, the low-frequency component was refractory to the number of repetitions. We observed a similar trend for the repetition-number-sensitive high-frequency component and less sensitive low-frequency component in several electrodes on the temporal cortex of both monkeys. Outside the temporal cortex we did not detect a similar frequency-dependent sensitivity that was specific to a region or consistent between the monkeys.

Figure 5 provides a summary of the relationship between the number of the stimulus repetitions and the strength of MMA (C and F), the response to Standard (A and D) stimuli, and the response to Deviant (B and E) stimuli in each monkey. As expected, in the population-level analysis (panel i in Figs 5C and F), MMA became larger with the increase in the number of repetitions in both monkeys (Friedman's test, $P < 0.0001$ in both monkeys, which survived FDR correction conducted across MMA and the responses to Standard and Deviant stimuli; $q = 0.05$). At the single-electrode level (panel ii), an effect of repetition number was observed ($P < 0.05$) in 20 and 42 electrodes for monkey C and for monkey Q, respectively. Among them, five and seven electrodes survived FDR correction ($q = 0.05$, represented by black lines in panel ii and black markers in panel iii). Likewise, the strength of the response to Deviant stimuli increased as a function of repetition number at the population level (panel i in Figs 5B and E, $P < 0.0001$ in both monkeys, which survived FDR correction) and in 10 and 36 electrodes ($P < 0.05$) for monkey C

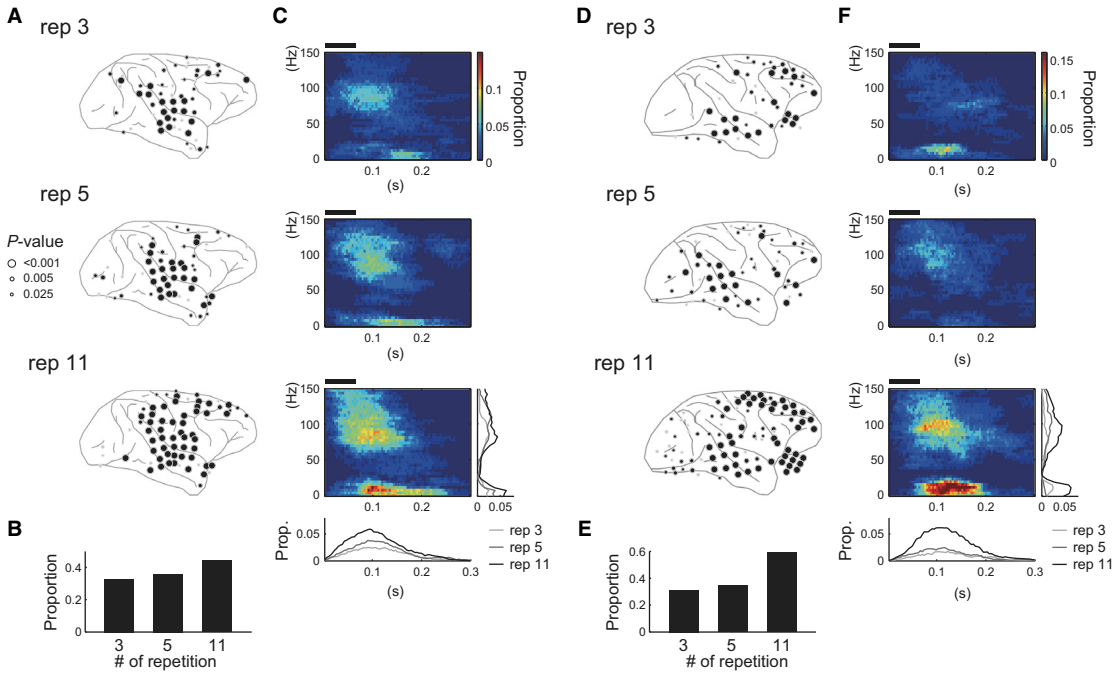

FIG. 3. Summary of the distribution of the electrodes exhibiting MMA. (A and D) Distribution of the electrodes with MMA on the cortical surfaces in (A) monkey C and (D) monkey Q. Each panel shows the spatial distribution of the electrodes with MMA in 3-, 5- and 11-repetitions conditions (top, middle and bottom panels, respectively). Black circles represent the electrodes surviving the correction for the multiple comparisons (FDR correction, $q = 0.05$) and gray circles represent the electrodes with $P < 0.025$. (B and E) The proportion of the electrodes with MMA in each condition. We counted the number of the electrodes that survived FDR correction. (C and F) The time–frequency pattern of MMA on average. We averaged the significant clusters across the electrodes surviving FDR correction. The black horizontal bar above each panel indicates the epoch when the tones were presented. The insets in the bottom panel show the frequency-collapsed (inset below the panel) or time-collapsed (inset on the right side of the panel) MMA pattern. Light gray, dark gray and black lines indicate the MMA in the condition of the 3-, 5- and 11-repetitions, respectively.

and monkey Q, respectively. Three and eight electrodes, respectively, survived FDR correction (panels ii and iii in Figs 5B and E). Note that we observed some electrodes on the temporal cortex that showed statistically robust increments of response to Deviant stimuli in both monkeys (black triangles in panel iii of Figs 5B and E). As for the response to Standard stimuli, the repetition-number effect was significant ($P < 0.0001$) at the population level in monkey Q (panel i in Fig. 5A) but not in monkey C ($P > 0.05$, panel i in Fig. 5D), although we observed a trend for a decrement in response at several electrodes with the increase in the repetition number. Eleven and twelve electrodes showed the repetition-number effect ($P < 0.05$) for monkeys C and Q, respectively, but none of them survived FDR correction (panel ii and iii in Figs 5A and D).

We designed the roving-oddball sequence so that the distributions of IDI were similar across Deviant stimuli after 3, 5 and 11 repetitions (Fig. 1C). To further confirm that larger responses to Deviant stimuli after more repetition were not due to the longer IDI and thus weaker SSA, we investigated the effect of IDI on the response strength to Deviant stimuli by calculating their correlation coefficient on a single-trial basis for each electrode (Fig. 6A). The length of IDI had little effect on the response strength, i.e. correlation coefficients were nearly zero in most electrodes (see the absolute values in Fig. 6). Taking the correlation coefficient as a measure for the effect of IDI, we also found that the IDI effect did not coincide with the facilitative repetition-number effect (Fig. 6B). While we observed the repetition-number effect in the electrodes on the temporal cortex in both subjects (triangles in Figs 5B and E), the relatively larger IDI effects were outside the temporal cortex (larger circles in Fig. 6C). We performed the same analysis for the time interval between Deviant and the latest presentation as Standard for a given stimulus and obtained similar results (data is not shown). Thus, we concluded that the stronger response to Deviant stimuli after more repetitions could not be attributed to SSA.

Repetition effect on cortical responsiveness

As shown in Fig. 3, we observed a spread of MMA as repetition number increased that involved a wide range of cortical regions. This raised the possibility that a sufficiently high number of repetitions can lead to activation of cortical regions that are not activated by auditory stimuli when they are presented with few or no preceding repetitive presentation of one stimulus. To test this, we examined the responsiveness of each electrode to Deviant stimuli and Control stimuli presented in random order without repetition (a schematic of the control sequence is shown in Fig. 7A), comparing the spectral powers before and after stimulus onset. We defined the electrodes that displayed a significant increment (Fig. 7) or decrement (Fig. 8) in spectral powers as 'responsive' electrodes. Note that we defined the responsiveness for Deviant and Control stimuli separately.

Figures 7B and D demonstrates which electrodes yielded a significant increment in the spectral power when the stimuli were presented as Control (panel i) and as Deviant (panels ii, iii and iv). Figs 7C and E (left panels) show the distribution of the electrodes with an increment in power to Deviant stimuli in at least one of the conditions, but not to Control stimuli (34 and 26 electrodes in monkeys C and Q, respectively). The electrodes responsive specifically to Deviant stimuli were observed over the dorsal part of the frontal cortex and the anterior part of the superior temporal gyrus in both

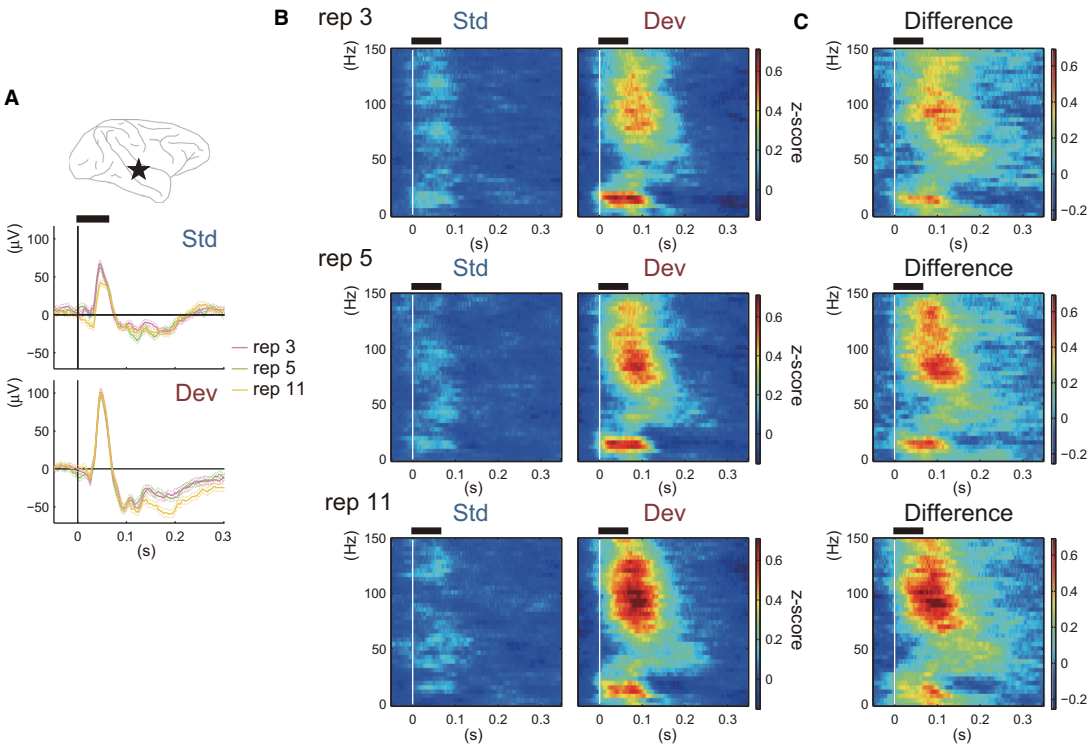

FIG. 4. An example of the responses to Standard and Deviant stimuli and the difference between them in each condition. (A) Location of an example electrode (top panel), ERPs in Standard trials (middle panel) and ERPs in Deviant trials (bottom panel). In the middle and bottom panels, purple, green and yellow lines indicate the 3-, 5- and 11-repetitions conditions, respectively. Dashed lines indicate the SE across the trials. (B) Responses to Standard (left column) and Deviant (right column) stimuli in the time–frequency domain. Each row indicates the responses in the 3- (top), 5- (middle) and 11- (bottom) repetitions condition. (C) The subtraction of the response to Standard stimuli from the response to Deviant stimuli. Black horizontal bar above each panel indicates the epoch when the tones were presented. Std, Standard; Dev, Deviant; rep, repetition number.

monkeys. The electrodes around the intraparietal sulcus showed a similar trend, although they did not survive the correction for multiple comparisons (FDR correction, $q = 0.05$) in monkey Q (gray circles in panel iv of Fig. 7D). The effect of repetition on responsiveness was most prominent when we compared the 11-repetitions condition (panel iv) with Control (panel i). Fifty-one and forty-six electrodes elicited a significant power increment to Deviant stimuli in the 11-repetitions condition, while 27 and 30 electrodes responded to Control for monkey C and for monkey Q, respectively. In monkey C, a repetition effect was also observed in the 3- and 5-repetitions conditions. A significant power increment was observed in 45 (3-repetitions) and 42 (5-repetitions) electrodes. In monkey Q, a repetition effect was not clear in the 3- or 5-repetitions conditions. Thirty-four electrodes showed an increment in the power ($P < 0.025$) in each condition, and 28 and 27 electrodes survived FDR correction in the 3- and 5- repetitions conditions, respectively. Figure 7F shows an example of the responses to Control and Deviant stimuli in each condition as recorded from one exemplar electrode on the frontal cortex (represented by a yellow circle with red edge in Fig. 7E). The left panel of Fig. 7F shows ERPs for Control and Deviant stimuli in the example electrode.

We also observed decrements in spectral power specific to Deviant stimuli (Fig. 8), although we could not discern a coherent pattern in the spatial distribution or repetition-number effect that was consistent between monkeys. The number of electrodes with a significant power decrement to Control and Deviant stimuli were 9, 10, 11 and 14 in monkey C and 12, 29, 23 and 21 in monkey Q. In each monkey, electrodes 17 and 33 showed a power decrement specifically to Deviant stimuli. These electrodes were scattered over the cortex; areas included the occipital and temporal cortices, the ventral premotor cortex and the area around the inferior parietal sulcus. The decrement in power started ~ 0.2 s after stimulus onset (right panel in Figs 8B and D), which is after MMA. Thus, the decrement in the power in these electrodes might be the result of MMA, which may influence cognitive functions (e.g., shift of attention, elevated arousal level) following change detection.

Discussion

The present study constitutes the first report on the stimulus-repetition effect on MMA and on the responses to Standard and Deviant stimuli, as determined by intracranial recording across cortical regions. In the time–frequency domain we found that, as the number of auditory stimulus repetitions increased, the cortical regions exhibiting MMA become more widely distributed. In addition, MMA became enhanced as a function of the number of stimulus repetitions, which was mainly due to augmentation of the response to Deviant stimuli. We also observed a small attenuation of the response to Standard stimuli. Additional analysis revealed that the stronger response to Deviants after more repetitions could be not explained by either the length of IDI or the time interval between Deviant and the latest presentation of Standard. Thus, we conclude that the facilitative repetition-number effect observed on the response to Deviant stimuli cannot be attributed to SSA. We further found that a subset of the electrodes outside the temporal cortex yielded a significant power increment only when the stimuli were

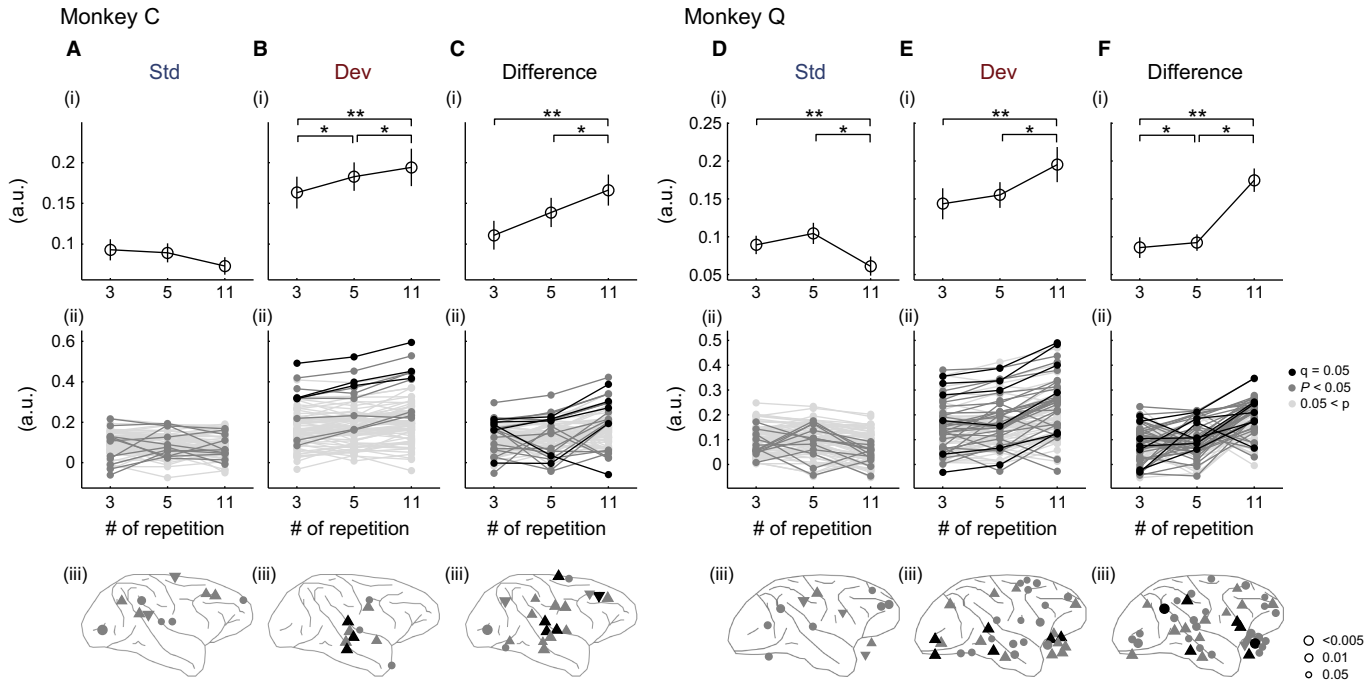

FIG. 5. Summary of the effect of repetition number on the response to Standard and Deviant stimuli and the difference between them (MMA). The relationship between repetition number and (A and D) the strength of the response to Standard stimuli, (B and E) the strength of the response to Deviant stimuli and (C and F) the strength of MMA in each monkey. The upper row shows the results at the population level. An effect of repetition number was significant for the response to Deviant stimuli and in MMA (panel i in B, C, E and F) in both monkeys (Friedman's test, all $P < 0.0001$, FDR correction, $q = 0.05$) and in the response to Standard stimuli in monkey Q (panel i in D; $P < 0.0001$). Horizontal bars represent the pairs showing significant differences in *post hoc* comparisons (sign-tests with FDR correction, $q = 0.05$). Vertical bars represent the 95% confidence interval. $*P < 0.005$, $**P < 0.001$. The middle row shows the results at the single-electrode level. Light gray lines indicate the electrodes with $P > 0.05$ (Friedman's test), dark gray lines indicate the electrodes with $P < 0.05$ and black lines indicate the electrodes surviving FDR correction ($q = 0.05$). The bottom row shows the distribution of the electrodes surviving FDR correction (black markers) and the electrodes with $P < 0.05$ (gray markers). Triangles and inverted triangles represent electrodes showing significant increases and decreases, respectively, in any one of the *post hoc* comparisons. Circles represent the electrodes exhibiting no significant difference in *post hoc* comparisons. Std, Standard; Dev, Deviant.

presented after sufficient repetition of one stimulus. Below, we will discuss our results with regard to previous findings, and the implications of our study to the current theoretical models of MMN.

Effect of the repetitive presentation of one stimulus

The present results seem compatible with the proposal by Javitt *et al.* (1996) that repetitive presentation of a stimulus enhances the response to different stimuli (e.g., Deviant). Literature on how the repetitive presentation of one stimulus affects processing of another stimulus is sparse. Several studies have demonstrated that intensive exposure to one stimulus leads to a decrement in the response to the adaptation or repetition stimulus (SSA) and reorganization of the stimulus-tuning properties in AI (Condon & Weinberger, 1991; Ulanovsky *et al.*, 2003; Parto Dezfouli & Daliri, 2015), primary visual cortex (Dragoi *et al.*, 2000; Ghisovan *et al.*, 2009) and MT (Kohn & Movshon, 2004). Additionally, some of these studies have reported an increased response to different stimuli (Dragoi *et al.*, 2000; Ulanovsky *et al.*, 2003). However, in these studies the adaptation stimulus was presented more than several hundred times or continuously over tens of seconds. Thus, their findings are not relevant to mechanisms underlying MMN–MMA. The present study demonstrates that 11 consecutive presentations of one stimulus is sufficient to facilitate the response to different stimuli at the neural population level, suggesting that there is a facilitative effect that serves as a neural mechanism for MMN–MMA. Although speculative, the repetition of one stimulus might induce short-term plasticity in synaptic efficacy in intrinsic and corticocortical circuits (Garrido *et al.*, 2009), priming the brain to be more responsive to stimuli other than the repeated one. Potential physiological mechanisms such as whether such plasticity occurs in a neuron-specific manner, as proposed by Javitt *et al.* (1996), remain to be investigated. One weakness of the present study is that the number of the repetitions and IDI co-varied. We concluded that the repetition-number effect could not be attributed to SSA because the IDI distributions were similar across conditions when we focused on stimuli with the same frequencies. However, if deviants exert a forward

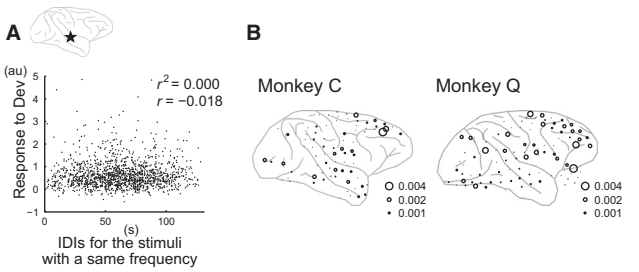

FIG. 6. IDI length cannot explain the repetition-number effect on the response to Deviant stimuli. (A) Scatter plot of the response strength to Deviants against IDI length. IDI length had little effect on the response to Deviants. (B) Distribution of the IDI effect. A stronger IDI effect did not coincide with the repetition-number effect in the response to Deviants.

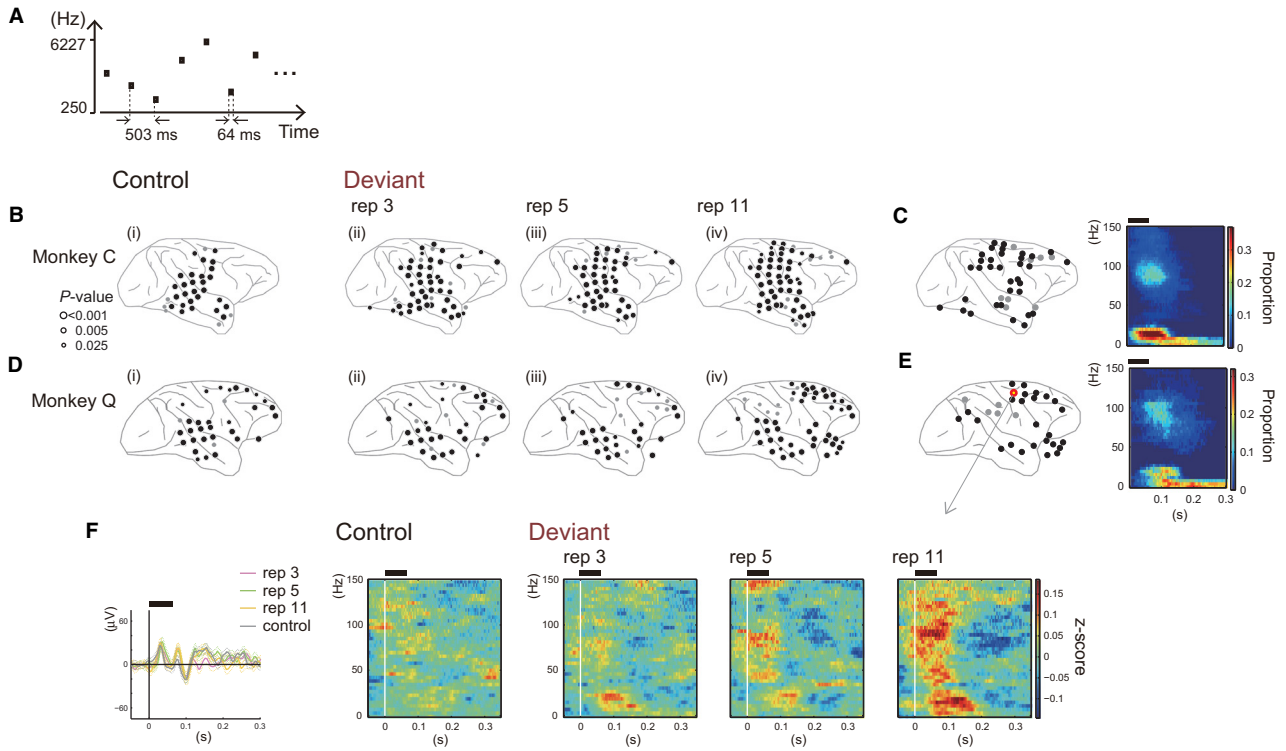

FIG. 7. Electrodes showing significant increments in spectral power after stimulus onset. (A) Schematic of the control sequence. The 20 types of stimuli comprising the roving-oddball sequence were presented in random order. (B and D) The distribution of the electrodes with significant increments in power after stimulus onset in the control sequence (panel i) or the presentation of the Deviant stimulus in the roving-oddball sequence (panels ii, iii and iv) in each monkey. Black circles represent the electrodes surviving FDR correction ($q = 0.05$) and dark circles represent the electrodes with $P < 0.025$. (C and E) The distribution of the electrodes showing a significant increment in power specifically to Deviant stimuli in any one of the conditions (left panel) and the time–frequency pattern of the power increment averaged across these electrodes (right panel). (F) An example of the response to Control and Deviant stimuli recorded from an electrode on the frontal cortex (represented by the yellow circle in the left panel of E). Black horizontal bars above the panels in C, E and F indicate the epoch when the tones were presented. Std, Standard; Dev, Deviant; rep, repetition number.

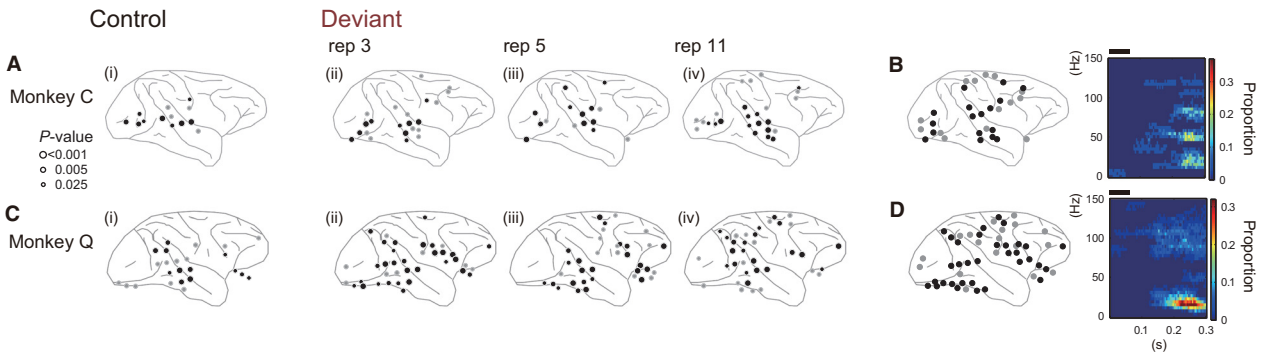

FIG. 8. Electrodes showing a significant decrement in the spectral power after stimulus onset. (A and C) The distribution of the electrodes with significant decrements in power after the stimulus onset in the control sequence (panel i) or the presentation of the Deviant stimulus in the roving-oddball sequence (panels ii, iii and iv). (B and D) The distribution of the electrodes showing significant decrements in power, specifically to Deviant stimuli, in any of the conditions (left panel), and the time–frequency pattern of the power decrement averaged across these electrodes (right panel). The format is the same as in Figure 7B–E. Std, Standard; Dev, Deviant; rep, repetition number.

suppressive effect on the cortical response regardless of the stimulus feature, the stronger deviant response after more repetition might be due to a longer IDI. A future study with a control sequence in which only the deviants are presented with the same IDIs as the roving-oddball sequence might be useful for testing this possibility, although we need to take into account the effect of the temporal predictability of the stimuli. In such a control sequence, stimulus presentation timing is unpredictable whereas in the roving-oddball sequence the stimuli are presented on a fixed-time interval and are thus temporally predictable.

Repetition effect in the temporal cortex

Our finding of repetition-number sensitivity in the temporal cortex comports with previous findings that neurons in the temporal cortex, specifically in AI, are sensitive to the presentation probability of

each stimulus in stimulus sequences (Ulanovsky *et al.*, 2003; von der Behrens *et al.*, 2009; Farley *et al.*, 2010; Taaseh *et al.*, 2011), or to the periodicity embedded in the sequence (Yaron *et al.*, 2012). Using subdural electrodes we demonstrated that the net activity of the neuronal populations residing in the temporal cortex can be modified by the statistical structure of the auditory stimulus sequence, similarly to neurons in AI, although the context of the effect in this study was opposite to the context in these previous works. While we found a context-dependent facilitative effect on the auditory response, the effect of the context emerged as suppression in the earlier studies. Given that AI is buried within the lateral sulcus in macaque monkeys, the activity observed at the electrodes on the temporal cortex is not likely to arise from AI. Subdural electrodes on the cortical surface, as in our study, cannot sample much signal from AI. Use of smaller and denser electrode arrays (Viventi *et al.*, 2011) would be helpful in examining which cortical regions contain a neuronal population that displays a stronger response to a Deviant stimulus when the preceding stimulus is repeated more times.

Possible factors explaining the discrepancies of this study from the previous studies in humans

Our results differed in several aspects from the findings of previous studies combining the roving-oddball sequence and EEG recording in human subjects (Baldeweg *et al.*, 2004; Haenschel *et al.*, 2005; Garrido *et al.*, 2009; Costa-Faidella *et al.*, 2011; Schmidt *et al.*, 2012). In previous studies, a repetition-number effect on the response to Standard stimuli, and/or on MMN, has been consistently demonstrated, while an effect on the response to Deviant stimuli was either not observed (Haenschel *et al.*, 2005; Costa-Faidella *et al.*, 2011) or was weaker than the effect on the response to Standard stimuli (Baldeweg *et al.*, 2004). For instance, in Baldeweg *et al.* (2004) the effect of the response to Deviant stimuli only became clear when the stimulus was repeated at least 18 times. In contrast we observed a remarkable effect on the response to Deviants after 11 preceding repetitive stimuli, and the repetition-number effect on the response to Standard was less robust. Below we deliberate on the possible factors that may explain these discrepancies.

Our observation of repetition-number effects on the response to Deviant stimuli, contrary to all previous studies except that of Baldeweg *et al.* (2004), may be due in part to differences in the recording modality. We recorded cortical activity with subdural electrodes while the previous studies used scalp electrodes. Recording with subdural electrodes can more specifically sample neural activity generated by the neuronal populations localized near the electrodes (~5 mm^2), a spatial resolution that cannot be attained by recording with scalp electrodes (Crone *et al.*, 2006; Buzsaki *et al.*, 2012). Indeed, a blurring or smearing effect of the skull has been repeatedly reported (Srinivasan *et al.*, 1996, 1998; van den Broek *et al.*, 1998; Wolters *et al.*, 2006) and EEG is thus considered to reflect net neural activity, i.e. the mixture of the signals coming from functionally divergent neuronal populations across cortical regions over 10 cm^2 (Srinivasan *et al.*, 1998). Thus, the signal of a small number of populations showing the repetition-number effect on the response to Deviant stimuli can be masked by the activity of other populations in the signal recorded from scalp electrodes.

Differences in the analytic approach between studies may also have a substantial impact. ERPs are much more reflective of low-frequency signals than higher ones. In extracellular field potentials, such as those in EEG and ECoG, the magnitude of spectral power scales as $1/f^n$ with n = 1–2 (Pritchard, 1992; Miller *et al.*, 2009). Calculation of ERPs does not include normalization procedures that cancel out the $1/f^n$ power scaling effect, thereby rendering low-frequency signals dominant. In contrast, spectrograms, such as those in this study, are generated by decomposition into and normalization at each frequency point, which enabled us to investigate activity in the high-frequency range (Fig. 4) and led to the finding of repetition-number sensitivity of the response to Deviant stimuli. Therefore, the absence of the repetition-number effect on the response to Deviants in the early studies might be due to the combination of scalp electrodes and analysis in ERPs.

While analysis of ERPs is not relevant for high-frequency signals, it can reveal other aspects of cortical evoked activity aside from changes in spectral powers, which may underlie discrepancies between studies concerning the repetition-number effect on the response to Standard. Importantly, neural events that are irrelevant to spectral-power changes presumably had a major effect in previous studies but were not statistically robust in our analyses. ERPs can be generated by spectral power changes and/or reset of the ongoing oscillatory activity such as the alpha and theta oscillations (Makeig *et al.*, 2002; Fell *et al.*, 2004; Fuentemilla *et al.*, 2006, 2008), which is observable in analysis of phase synchronization across trials. Moreover, a prior EEG study has demonstrated that MMN in the scalp frontal electrodes arise from a combination of power changes and phase reset of low-frequency signals (Fuentemilla *et al.*, 2008). Thus, the amplitude of MMN in the scalp frontal electrode is likely to depend on both the strength of power changes and phase reset. We therefore might have underestimated the repetition-number effect on the response to Standard stimuli, because we focused our analysis on spectrograms that represent only the spectral power changes. Additionally, the cluster analysis (Maris & Oostenveld, 2007) we adopted detected only one component that yielded a statistically most robust difference between Standard and Deviant trials in the spectrogram. Thus, it is possible that we have overlooked components showing response attenuation to Standard stimuli with the increase in the number of repetitions.

We also need to consider the possibility of species differences. Several studies have discussed the similarities of MMN-like activity in non-human primates to MMN in humans (Javitt *et al.*, 1992; Ueno *et al.*, 2008; Gil-da-Costa *et al.*, 2013; Komatsu *et al.*, 2015), but they were different between species when examined using an oddball sequence with more abstract stimulus features (Honing *et al.*, 2012). Further studies in non-human primates involving more subjects and analysis using the grand-average ERP across subjects, with special focus on a specific ERP component, as in studies in humans, would be helpful in settling this issue.

MMA in the frontal cortex

We observed a repetition-number effect on MMA both inside and outside the temporal cortex. With the increase in the repetition number, MMA occurred in more widely distributed electrodes on the frontal and parietal cortices. These regions contained electrodes that yielded a spectral power increment only after sufficient repetition of one stimulus. Considering these finding in conjunction with the observation that the response to Deviant stimuli in the temporal cortex grew as a function of repetition number, the most straightforward interpretation of these data is that only when a stimulus was repeated sufficiently was the response of the temporal cortex to a Deviant stimulus vigorous enough to trigger a cascade of corticocortical interactions resulting in a widely distributed MMA involving the frontal and parietal cortices. The idea that the frontal cortex is

driven by Deviant stimuli only when the preceding stimulus is repeated many times comports with the finding by Sato *et al.* (2000) that the frontal MMN generator becomes active only when the probability of the Standard was sufficiently high (> 90%) in the oddball sequence.

Frontal cortex involvement in MMN has been suggested by other studies with different analytic methods and/or recording modalities (Giard *et al.*, 1990; Deouell *et al.*, 1998; Muller *et al.*, 2002; Molholm *et al.*, 2005; Boly *et al.*, 2011) but, within the large body of literature concerning MMN, studies showing frontal MMN are in the minority (Deouell, 2007). This might be partially because of insufficient repetition number. Although we have speculated that the frontal cortex is a downstream component of corticocortical cascades, the precise role of the frontal cortex in MMN generation remains an open question. Garrido *et al.* (2009) suggested that changes in synaptic efficacy through repetition within AI, and between AI and another region, underlies MMN. The frontal cortex might be involved in such plastic changes of corticocortical connectivity. Further analysis to estimate the functional and directional connectivity measures among the electrodes would reveal dynamic changes both in bottom-up and top-down signal flow involving the frontal cortex and provide new insights into the functional role of the frontal cortex in the generation of MMN.

Implications for existing models of MMN

The aim of the present study was to test the stimulus-repetition effect proposed by Javitt *et al.* (1996). While we do not intend to commit to or challenge any theoretical models for MMN in humans based on our findings, they do have some potential implications for improving the current models.

May & Tiitinen (2010) proposed the 'adaptation model' of MMN in which the change-detection mechanism would rely on changes in synaptic connectivity through repetition, or through adaptation to one stimulus. They further postulated that MMN is the resultant modification of an auditory-evoked response known as N1, which is observable irrespective of context and is associated with the obligatory processing of auditory signals. Jaaskelainen *et al.* (2004) provided evidence in support of this idea in demonstrating the same source of MMN and N1 in the human auditory cortex. Several recent studies have explored deviant-specific neuronal activity other than the obligatory response with combination of the oddball sequence and many-standards condition, but did not observe such activity in macaque sensory cortices (Fishman & Steinschneider, 2012; Kaliukhovich & Vogels, 2014) or in the human auditory association cortex (Eliades *et al.*, 2014). Whether or not the many-standards condition is relevant for investigating the obligatory auditory response is still debatable. Practically, however, it allows us to present stimuli physically identical to the Deviants by maintaining equal probability, but in a different context. Our finding that a subset of the electrodes on the frontal cortex showed a spectral power increment to Deviant stimuli only after sufficient repetition of one stimulus suggests the possibility that deviant-specific activity exists outside the sensory cortices. MMN might be generated by neural mechanisms different from the obligatory auditory processing and instead involve a wide range of cortical regions outside the sensory cortex. Thus, while our findings argue for a significant role of adaptation, they suggest that MMN might be generated from a neural mechanism that is different from N1 and involves areas outside the temporal cortex. However, further studies are required to fill the gaps in human and non-human primate studies.

The adaptation model is often contrasted with the memory-based (Naatanen *et al.*, 2012) or predictive coding (Friston, 2005) model of MMN. These models propose that MMN arises through a process that compares the incoming sensory input with the memory trace of the Standard stimulus or with a prediction signal endogenously generated in the brain. The comparison process might be implemented by the afferent input carrying the information of Deviant stimulus into a cortical circuit in which synaptic connectivity has already changed through adaptation. Future studies investigating what neural phenomena occur during the repetition of a Standard stimulus in inter-areal signal flows and synaptic efficacy might lead to integration of the above models.

Conclusions

Our results show that the repetitive presentation of one stimulus facilitates the response of the brain to the other stimuli, involving widespread cortical regions such as the frontal and parietal cortices, thereby implying that the repetitive presentation of one stimulus primes the brain to deploy more resources to the stimuli breaking the regularity. The facilitative effect of the stimulus repetition may contribute to the generation of MMN-like scalp potential in non-human primates that are expected to be an animal model of MMN in humans.

Conflict of interest

The authors have no conflict of interests to declare.

Acknowledgements

We are grateful to Naomi Hasegawa and Tomonori Notoya for providing veterinary care and technical support. This work was supported by the Brain Science Project of the Center for Novel Science Initiatives (CNSI), National institute of Natural Science (NINS; Grant Number BS261006), and Ministry of Education, Culture, Sports, Science, and Technology Grant in Aid for Scientific Research on Innovative Areas (21118002). The National BioResource Project 'Japanese monkey' provided monkey C.

Abbreviations

AI, primary auditory cortex; ECoG, electrocorticogram; EEG, electroencephalogram; ERP, event-related potential; FDR, false-discovery rate; IDI, inter-deviant time interval; MMA, mismatch activity; MMN, mismatch negativity; MRI, magnetic resonance image; SSA, stimulus-specific adaptation.

References

Antunes, F.M., Nelken, I., Covey, E. & Malmierca, M.S. (2010) Stimulus-specific adaptation in the auditory thalamus of the anesthetized rat. *PLoS One*, **5**, e14071.

Baldeweg, T., Klugman, A., Gruzelier, J. & Hirsch, S.R. (2004) Mismatch negativity potentials and cognitive impairment in schizophrenia. *Schizophr. Res.*, **69**, 203–217.

von der Behrens, W., Bauerle, P., Kossl, M. & Gaese, B.H. (2009) Correlating stimulus-specific adaptation of cortical neurons and local field potentials in the awake rat. *J. Neurosci.*, **29**, 13837–13849.

Benjamini, Y. & Hochberg, Y. (1995) Controlling the false discovery rate – a practical and powerful approach to multiple testing. *J. Roy. Stat. Soc. B. Met.*, **57**, 289–300.

Boly, M., Garrido, M.I., Gosseries, O., Bruno, M.A., Boveroux, P., Schnakers, C., Massimini, M., Litvak, V., Laureys, S. & Friston, K. (2011) Response to Comment on "Preserved feedforward but impaired top-down processes in the vegetative state". *Science*, **334**, 1203.

Brainard, D.H. (1997) The psychophysics toolbox. *Spatial Vision*, **10**, 433–436.

van den Broek, S.P., Reinders, F., Donderwinkel, M. & Peters, M.J. (1998) Volume conduction effects in EEG and MEG. *Electroen. Clin. Neuro.*, **106**, 522–534.

Buzsaki, G., Anastassiou, C.A. & Koch, C. (2012) The origin of extracellular fields and currents–EEG, ECoG, LFP and spikes. *Nat. Rev. Neurosci.*, **13**, 407–420.

Condon, C.D. & Weinberger, N.M. (1991) Habituation produces frequency-specific plasticity of receptive fields in the auditory cortex. *Behav. Neurosci.*, **105**, 416–430.

Costa-Faidella, J., Baldeweg, T., Grimm, S. & Escera, C. (2011) Interactions between "what" and "when" in the auditory system: temporal predictability enhances repetition suppression. *J. Neurosci.*, **31**, 18590–18597.

Crone, N.E., Sinai, A. & Korzeniewska, A. (2006) High-frequency gamma oscillations and human brain mapping with electrocorticography. *Prog. Brain Res.*, **159**, 275–295.

Deouell, L.Y. (2007) The frontal generator of the mismatch negativity revisited. *J. Psychophysiol.*, **21**, 188–203.

Deouell, L.Y., Bentin, S. & Giard, M.H. (1998) Mismatch negativity in dichotic listening: evidence for interhemispheric differences and multiple generators. *Psychophysiology*, **35**, 355–365.

Desimone, R. (1996) Neural mechanisms for visual memory and their role in attention. *P. Natl Acad. Sci. USA*, **93**, 13494–13499.

Dragoi, V., Sharma, J. & Sur, M. (2000) Adaptation-induced plasticity of orientation tuning in adult visual cortex. *Neuron*, **28**, 287–298.

Eliades, S.J., Crone, N.E., Anderson, W.S., Ramadoss, D., Lenz, F.A. & BoatmanReich, D. (2014) Adaptation of high-gamma responses in human auditory association cortex. *J. Neurophysiol.*, **112**, 2147–2163.

Farley, B.J., Quirk, M.C., Doherty, J.J. & Christian, E.P. (2010) Stimulus-specific adaptation in auditory cortex is an NMDA-independent process distinct from the sensory novelty encoded by the mismatch negativity. *J. Neurosci.*, **30**, 16475–16484.

Fell, J., Dietl, T., Grunwald, T., Kurthen, M., Klaver, P., Trautner, P., Schaller, C., Elger, C.E. & Fernandez, G. (2004) Neural bases of cognitive ERPs: more than phase reset. *J. Cognitive Neurosci.*, **16**, 1595–1604.

Fishman, Y.I. & Steinschneider, M. (2012) Searching for the mismatch negativity in primary auditory cortex of the awake monkey: deviance detection or stimulus specific adaptation? *J. Neurosci.*, **32**, 15747–15758.

Friston, K. (2005) A theory of cortical responses. *Philos. T. Roy. Soc. B.*, **360**, 815–836.

Fruhstorfer, H., Soveri, P. & Jarvilehto, T. (1970) Short-term habituation of the auditory evoked response in man. *Electroen. Clin. Neuro.*, **28**, 153–161.

Fuentemilla, L., Marco-Pallares, J. & Grau, C. (2006) Modulation of spectral power and of phase resetting of EEG contributes differentially to the generation of auditory event-related potentials. *NeuroImage*, **30**, 909–916.

Fuentemilla, L., Marco-Pallares, J., Munte, T.F. & Grau, C. (2008) Theta EEG oscillatory activity and auditory change detection. *Brain Res.*, **1220**, 93–101.

Garrido, M.I., Kilner, J.M., Kiebel, S.J., Stephan, K.E., Baldeweg, T. & Friston, K.J. (2009) Repetition suppression and plasticity in the human brain. *NeuroImage*, **48**, 269–279.

Ghisovan, N., Nemri, A., Shumikhina, S. & Molotchnikoff, S. (2009) Long adaptation reveals mostly attractive shifts of orientation tuning in cat primary visual cortex. *Neuroscience*, **164**, 1274–1283.

Giard, M.H., Perrin, F., Pernier, J. & Bouchet, P. (1990) Brain generators implicated in the processing of auditory stimulus deviance: a topographic event-related potential study. *Psychophysiology*, **27**, 627–640.

Gil-da-Costa, R., Stoner, G.R., Fung, R. & Albright, T.D. (2013) Nonhuman primate model of schizophrenia using a noninvasive EEG method. *P. Natl Acad. Sci. USA*, **110**, 15425–15430.

Haenschel, C., Vernon, D.J., Dwivedi, P., Gruzelier, J.H. & Baldeweg, T. (2005) Event-related brain potential correlates of human auditory sensory memory-trace formation. *J. Neurosci.*, **25**, 10494–10501.

Honing, H., Merchant, H., Haden, G.P., Prado, L. & Bartolo, R. (2012) Rhesus monkeys (*Macaca mulatta*) detect rhythmic groups in music, but not the beat. *PLoS One*, **7**, e51369.

Jaaskelainen, I.P., Ahveninen, J., Bonmassar, G., Dale, A.M., Ilmoniemi, R.J., Levanen, S., Lin, F.H., May, P., Melcher, J., Stufflebeam, S., Tiitinen, H. & Belliveau, J.W. (2004) Human posterior auditory cortex gates novel sounds to consciousness. *P. Natl Acad. Sci. USA*, **101**, 6809–6814.

Jacobsen, T. & Schroger, E. (2001) Is there pre-attentive memory-based comparison of pitch? *Psychophysiology*, **38**, 723–727.

Javitt, D.C., Schroeder, C.E., Steinschneider, M., Arezzo, J.C. & Vaughan, H.G. Jr (1992) Demonstration of mismatch negativity in the monkey. *Electroen. Clin. Neuro.*, **83**, 87–90.

Javitt, D.C., Steinschneider, M., Schroeder, C.E., Vaughan, H.G. Jr & Arezzo, J.C. (1994) Detection of stimulus deviance within primate primary auditory cortex: intracortical mechanisms of mismatch negativity (MMN) generation. *Brain Res.*, **667**, 192–200.

Javitt, D.C., Steinschneider, M., Schroeder, C.E. & Arezzo, J.C. (1996) Role of cortical N-methyl-D-aspartate receptors in auditory sensory memory and mismatch negativity generation: implications for schizophrenia. *P. Natl Acad. Sci. USA*, **93**, 11962–11967.

Kaliukhovich, D.A. & Vogels, R. (2014) Neurons in macaque inferior temporal cortex show no surprise response to deviants in visual oddball sequences. *J. Neurosci.*, **34**, 12801–12815.

Kayser, C., Petkov, C.I. & Logothetis, N.K. (2007) Tuning to sound frequency in auditory field potentials. *J. Neurophysiol.*, **98**, 1806–1809.

Kohn, A. & Movshon, J.A. (2004) Adaptation changes the direction tuning of macaque MT neurons. *Nat. Neurosci.*, **7**, 764–772.

Komatsu, M., Takaura, K. & Fujii, N. (2015) Mismatch negativity in common marmosets: whole-cortical recordings with multi-channel electrocorticograms. *Sci. Rep.*, **5**, 15006.

Makeig, S., Westerfield, M., Jung, T.P., Enghoff, S., Townsend, J., Courchesne, E. & Sejnowski, T.J. (2002) Dynamic brain sources of visual evoked responses. *Science*, **295**, 690–694.

Malmierca, M.S., Cristaudo, S., Perez-Gonzalez, D. & Covey, E. (2009) Stimulus-specific adaptation in the inferior colliculus of the anesthetized rat. *J. Neurosci.*, **29**, 5483–5493.

Maris, E. & Oostenveld, R. (2007) Nonparametric statistical testing of EEG- and MEG-data. *J. Neurosci. Meth.*, **164**, 177–190.

May, P.J. & Tiitinen, H. (2010) Mismatch negativity (MMN), the deviance-elicited auditory deflection, explained. *Psychophysiology*, **47**, 66–122.

Miller, K.J., Zanos, S., Fetz, E.E., den Nijs, M. & Ojemann, J.G. (2009) Decoupling the cortical power spectrum reveals real-time representation of individual finger movements in humans. *J. Neurosci.*, **29**, 3132–3137.

Mitra, P. & Bokil, H. (2008) *Observed brain dynamics*. Oxford University Press, Oxford, New York.

Molholm, S., Martinez, A., Ritter, W., Javitt, D.C. & Foxe, J.J. (2005) The neural circuitry of pre-attentive auditory change-detection: an fMRI study of pitch and duration mismatch negativity generators. *Cereb. Cortex*, **15**, 545–551.

Muller, B.W., Juptner, M., Jentzen, W. & Muller, S.P. (2002) Cortical activation to auditory mismatch elicited by frequency deviant and complex novel sounds: a PET study. *NeuroImage*, **17**, 231–239.

Naatanen, R., Gaillard, A.W. & Mantysalo, S. (1978) Early selective-attention effect on evoked potential reinterpreted. *Acta Psychol.*, **42**, 313–329.

Naatanen, R., Kujala, T., Escera, C., Baldeweg, T., Kreegipuu, K., Carlson, S. & Ponton, C. (2012) The mismatch negativity (MMN)–a unique window to disturbed central auditory processing in ageing and different clinical conditions. *Clin. Neurophysiol.*, **123**, 424–458.

Nagasaka, Y., Shimoda, K. & Fujii, N. (2011) Multidimensional recording (MDR) and data sharing: an ecological open research and educational platform for neuroscience. *PLoS One*, **6**, e22561.

Parto Dezfouli, M. & Daliri, M.R. (2015) The effect of adaptation on the tuning curves of rat auditory cortex. *PLoS One*, **10**, e0115621.

Pelli, D.G. (1997) The VideoToolbox software for visual psychophysics: transforming numbers into movies. *Spatial Vision*, **10**, 437–442.

Perez-Gonzalez, D., Malmierca, M.S. & Covey, E. (2005) Novelty detector neurons in the mammalian auditory midbrain. *Eur. J. Neurosci.*, **22**, 2879–2885.

Pritchard, W.S. (1992) The brain in fractal time: 1/f-like power spectrum scaling of the human electroencephalogram. *Int. J. Neurosci.*, **66**, 119–129.

Ray, S. & Maunsell, J.H. (2011) Different origins of gamma rhythm and high-gamma activity in macaque visual cortex. *PLoS Biol.*, **9**, e1000610.

Ray, S., Crone, N.E., Niebur, E., Franaszczuk, P.J. & Hsiao, S.S. (2008) Neural correlates of high-gamma oscillations (60-200 Hz) in macaque local field potentials and their potential implications in electrocorticography. *J. Neurosci.*, **28**, 11526–11536.

Sato, Y., Yabe, H., Hiruma, T., Sutoh, T., Shinozaki, N., Nashida, T. & Kaneko, S. (2000) The effect of deviant stimulus probability on the human mismatch process. *NeuroReport*, **11**, 3703–3708.

Schmidt, A., Bachmann, R., Kometer, M., Csomor, P.A., Stephan, K.E., Seifritz, E. & Vollenweider, F.X. (2012) Mismatch negativity encoding of prediction errors predicts S-ketamine-induced cognitive impairments. *Neuropsychopharmacology*, **37**, 865–875.

Srinivasan, R., Nunez, P.L., Tucker, D.M., Silberstein, R.B. & Cadusch, P.J. (1996) Spatial sampling and filtering of EEG with spline laplacians to estimate cortical potentials. *Brain Topogr.*, **8**, 355–366.

Srinivasan, R., Nunez, P.L. & Silberstein, R.B. (1998) Spatial filtering and neocortical dynamics: estimates of EEG coherence. *IEEE T. Biomed. Eng.*, **45**, 814–826.

Taaseh, N., Yaron, A. & Nelken, I. (2011) Stimulus-specific adaptation and deviance detection in the rat auditory cortex. *PLoS One*, **6**, e23369.

Ueno, A., Hirata, S., Fuwa, K., Sugama, K., Kusunoki, K., Matsuda, G., Fukushima, H., Hiraki, K., Tomonaga, M. & Hasegawa, T. (2008) Auditory ERPs to stimulus deviance in an awake chimpanzee (Pan troglodytes): towards hominid cognitive neurosciences. *PLoS One*, **3**, e1442.

Ulanovsky, N., Las, L. & Nelken, I. (2003) Processing of low-probability sounds by cortical neurons. *Nat. Neurosci.*, **6**, 391–398.

Viventi, J., Kim, D.H., Vigeland, L., Frechette, E.S., Blanco, J.A., Kim, Y.S., Avrin, A.E., Tiruvadi, V.R., Hwang, S.W., Vanleer, A.C., Wulsin, D.F., Davis, K., Gelber, C.E., Palmer, L., Van der Spiegel, J., Wu, J., Xiao, J., Huang, Y., Contreras, D., Rogers, J.A. & Litt, B. (2011) Flexible, foldable, actively multiplexed, high-density electrode array for mapping brain activity in vivo. *Nat. Neurosci.*, **14**, 1599–1605.

Wolters, C.H., Anwander, A., Tricoche, X., Weinstein, D., Koch, M.A. & MacLeod, R.S. (2006) Influence of tissue conductivity anisotropy on EEG/MEG field and return current computation in a realistic head model: a simulation and visualization study using high-resolution finite element modeling. *NeuroImage*, **30**, 813–826.

Yaron, A., Hershenhoren, I. & Nelken, I. (2012) Sensitivity to complex statistical regularities in rat auditory cortex. *Neuron*, **76**, 603–615.